Exp. Theo. NANOTECHNOLOGY 10 (2026) 887-906 https://doi.org/10.56053/10.S.887

Application of extended Weibull distribution and triangular function for optimizing electrical parameters of solar cells with nanotechnology-enhanced modeling and nanoscale optimization approaches

M. S. Ibrahim[1,], Tarik T. Issa[2], Bilal Yaqoob[3], Etmad Naji Fayyadh[4], Ahmed Rashid[5], Ruqaya Shaker Mahmood[6]*

[1]College of Applied Sciences, University of Technology- Iraq, Baghdad, Iraq
[2]Department of Radiology and Sonar, College of Medical and Health Technology, Gilgamesh University, Baghdad, Iraq
[3, 5]College of Arts, Al-Iraqia University, Baghdad, Iraq
[4]Continuing Education Center, University of Fallujah, Ramadi, Iraq
[6]Applied Sciences Department, University of Technology- Iraq, Baghdad, Iraq
[*]) Email: ahmedsiham739@gmail.com

Received 3/3/2026, *Received in revised form* 29/3/2026, *Accepted* 18/4/2026, *Published* 15/5/2026

Efficiency and reliability enhancement in solar cell technology is essential for accelerating the global transition toward sustainable and renewable energy systems. This study focuses on optimizing the key electrical parameters of solar cells—short-circuit current density (Jsc), open-circuit voltage (Voc), fill factor (FF), and efficiency (η)—to improve performance under varying environmental conditions. To achieve this, the Extended Weibull Distribution and the Triangular Function are employed as robust analytical tools. The Extended Weibull Distribution effectively captures the stochastic and temperature-dependent behavior of solar cell performance, allowing accurate statistical modeling and reliable parameter extraction. In parallel, the Triangular Function is used to model I–V characteristics due to its simplicity and ability to approximate nonlinear behavior while reducing computational complexity. Experimental and computational analyses confirm the effectiveness of the proposed approach. Temperature-dependent results reveal that efficiency reaches a maximum of 0.55 with high reliability (0.94) at 5 °C, decreases at moderate temperatures, and exhibits fluctuating efficiency and reliability at higher temperatures, highlighting temperature sensitivity as a critical performance factor.

Furthermore, the integration of the fuzzy set method enhances reliability analysis by accounting for uncertainty and variability in operating conditions. The fuzzy approach provides a flexible reliability range, from 0.99 at low temperatures to 0.81 at 70 °C, complementing traditional statistical methods. Overall, this comprehensive framework offers valuable insights for developing more efficient, reliable, and adaptable solar cells for real-world applications. In addition, nanotechnology-based approaches, including nanoscale material engineering and nano-enabled modeling techniques, can further enhance parameter optimization, improve charge transport, and increase the overall efficiency and reliability of solar cells under varying environmental conditions.

Keywords: Weibull distribution; Solar cells; Triangular function; Reliability; Nanotechnology.

1. INTRODUCTION

Solar power is increasingly recognized as a cornerstone of the global transition toward environmental sustainability and energy security, owing to its ability to meet growing energy demands while significantly reducing greenhouse gas emissions [1]. The effectiveness of solar energy systems is strongly dependent on solar cell efficiency and performance, which directly influence the economic viability and large-scale adoption of this technology [2]. Consequently, extensive research has focused on improving the efficiency and reliability of solar cells through optimization of their electrical characteristics [3]. This study addresses existing performance limitations by proposing an advanced parameter extraction framework based on the Extended Weibull Distribution and the Triangular Function [4]. Key electrical parameters—including short-circuit current density (Jsc), open-circuit voltage (Voc), fill factor (FF), and efficiency (η)—play a decisive role in determining overall solar cell performance under real operating conditions [5]. These parameters are influenced by material properties, device architecture, and environmental factors such as temperature and irradiation [6]. Conventional parameter extraction methods are often complex, computationally intensive, and insufficiently robust in handling variability and uncertainty [7]. In contrast, statistical and mathematical models provide more flexible and accurate alternatives [8]. The Weibull Distribution is widely applied in reliability engineering and life data analysis due to its versatility in modeling uncertainty and variability [9, 10]. The Extended Weibull Distribution enhances this capability by introducing additional parameters, enabling more accurate representation of the probabilistic behavior of solar cells under diverse operating conditions [11, 12]. Its adaptability makes it particularly suitable for solar cell performance evaluation. Complementarily, the Triangular Function offers a simple yet effective means of approximating nonlinear relationships, especially the current–voltage (I–V) characteristics of solar cells [13–16]. By integrating the Extended Weibull Distribution with the Triangular Function, this study presents a novel and efficient framework for extracting electrical parameters with improved precision and reduced computational complexity [17, 18]. Experimental and computational validations demonstrate enhanced accuracy in parameter estimation and reliability assessment. The proposed approach provides a robust and adaptable methodology for optimizing solar cell efficiency and reliability, with significant implications for both academic research and industrial applications, thereby supporting the broader goal of sustainable renewable energy development [19, 20]. Recent advances in nanotechnology have significantly contributed to improving solar cell performance through nanoscale material engineering and enhanced charge transport mechanisms. Nanostructured materials, such as quantum dots, nanowires, and thin-film nanolayers, enable better light absorption, reduced recombination losses, and improved electrical conductivity. Integrating nanotechnology with statistical and mathematical modeling provides a powerful framework for optimizing solar cell efficiency and reliability.

2. EXTENDED WEIBULL DISTRIBUTION

A two-or three-parameter Weibull distribution is possible. Parameters for both the shape and the scale are the two most important ones. A third parameter, the location or threshold parameter may also be included. This leads us to the following description of the two-parameter Weibull distribution's purpose [21];

$$F(x) = \frac{\beta x}{\alpha^{\beta}} \mathrm{e}^{\left[\left(\frac{x}{\alpha}\right)^{\beta}\right]}, 0 \le x \le \infty \quad (1)$$

where the shape parameter is β>0 and the scale parameter is α>0

Also, the Weibull distrubution function with three parameters is as follows [22]

$$f(x) = \frac{\beta(x-\gamma)^{\beta-1}}{\alpha^{\beta}} \mathrm{e}^{-\left[\left(\frac{x-\gamma}{\alpha}\right)^{\beta}\right]}, \gamma < x < \infty \quad (2)$$

Since the shape parameter is β>0, the scale parameter is α>0, and the position parameter is γ≥0, the two-parameter and three-parameter Weibull quadratic can be used to find a new distribution, which is the mixed Weibull distribution, whose function takes different forms. Find the mixed Weibull distribution.

2.1. Finding mixture weibull distribution

To find a mixed Weibull distribution, there must be a new parameter or parameters to link the distributions together, and these parameters are the mixing parameters (w_i) and $\sum_{i=1}^{n} w_i = 1$. The number of mixing parameters is equivalent to the number of components or distributions used, minus one, for the purpose of determining the percentage contribution of each component or distribution in the mixed distribution, whether these distributions are of the same type or of different types. In general, the Probability Density Function for the mixed distribution will be as follows [23];

$$f(x) = w_1 f_1(x) + w_1 f_1(x) + w_1 f_1(x) \ldots + w_n f_n(x) \quad (3)$$

where f(x) represents the probability density function of the mixed distribution, i=1…..n, wi is the mixing parameter and $f_1(x), f_2(x), \ldots, f_n(x)$ they are the probability density functions of the distributions contributing to the mixed distribution. Also, the Cumulative Distribution Function for the mixed distribution is as follows [24]

$$F(x) = w_1 F_1(x) + w_2 F_2(x) + \ldots + w_n F_n(x) \quad (4)$$

where F(x) represents the aggregate distribution function of the mixed distribution and $F_1(x)$, $F_2(x), \ldots, F_n(x)$ are the aggregate distribution functions of the distributions contributing to the mixed distribution. The Survival or Function or Reliability function for the mixed distribution will be written as follows [25]

$$R(x) = w_1 R_1(x) + w_2 R_2(x) + \ldots + w_n R_n(x) \quad (5)$$

in where R(x) stands for the mixed distribution's survival function and R_1 (x), R_2 (x),..., R_n (x) are the distributions' survival functions that make up the mixed distribution. For the mixed distribution, the Hazard Function or Failure Rate will look like this: [26]

$$h(x) = w_1 h_1(x) + w_2 h_2(x) + \ldots + w_n h_n(x) \quad (6)$$

where h(x) represents the survival function for the mixed distribution and $h_1(x), h_2(x), \ldots, h_n(x)$ are the hazard functions for the distributions contributing to the mixed distribution.

In our research, we will focus on the case of mixing the two Weibull distributions, one with two parameters and the other with three parameters, using the mixing parameter (w), which represents the percentage contribution of each component (distribution) to the mixed Weibull distribution. Different values will be given for the mixing parameter through which the Weibull distribution functions are calculated (mixed). The probability density function for the mixed distribution for this case is [27]:

$$f(x) = wf_1(x) + (1-w)f_2(x) \quad (7)$$

where f_1 (x) represents the two-parameter Weibull distribution function, f_2 (x) represents the three-parameter Weibull distribution function, and w represents the mixing parameter. From equations (1) and (2) we obtain the probability density function for the mixed Weibull distribution

$$f(x) = w\left[\frac{\beta_1(x)^{\beta_1-1}}{\alpha_1{}^{\beta_1}} \mathrm{e}^{-\left[\left(\frac{x}{\alpha_1}\right)^{\beta_1}\right]}\right] + (1-w)\left[\frac{\beta_2(x)^{\beta_2-1}}{\alpha_2{}^{\beta_2}} \mathrm{e}^{-\left[\left(\frac{x}{\alpha_2}\right)^{\beta_2}\right]}\right] \quad (8)$$

In the same way, the aggregate distribution function for the mixed distribution is [28]:

$$F(x) = wF_1(x) + (1-w)F_2(x) \quad (9)$$

Since the aggregate distribution function of the two-parameter Weibull distribution is [29]

$$F_1(x) = 1 - \mathrm{e}^{-\left[\left(\frac{\mathrm{x}^{\beta_1}}{\alpha_1}\right)\right]} \quad (10)$$

The aggregate distribution function of the three-parameter Weibull distribution is [30]

$$F_2(x) = 1 - \mathrm{e}^{-\left[\left(\frac{(x-\gamma)^{\beta_2}}{\alpha_2}\right)\right]} \quad (11)$$

Therefore, the aggregate distribution function for the mixed Weibull distribution will be as follows [31]

$$F(x) = w\left[1 - \mathrm{e}^{-\left[\left(\frac{\mathrm{x}^{\beta_1}}{\alpha_1}\right)\right]}\right] + (1-w)\left[1 - \mathrm{e}^{-\left[\left(\frac{(x-\gamma)^{\beta_2}}{\alpha_2}\right)\right]}\right] \quad (12)$$

Also, the survival function for the mixed distribution is [32]

$$R(x) = wR_1(x) + (1-w)R_2(x) \quad (13)$$

Since the $R(x) = 1 - F(x)$

The survival function for a two-parameter Weibull distribution is [33]

$$R_1(x) = \mathrm{e}^{-\left[\left(\frac{\mathrm{x}^{\beta_1}}{\alpha_1}\right)\right]} \quad (14)$$

The survival function of the three-parameter Weibull distribution is [34]

$$R_2(x) = \mathrm{e}^{-\left[\left(\frac{(x-\gamma)^{\beta_2}}{\alpha_2}\right)\right]} \quad (15)$$

Therefore, the survival function for the mixed Weibull distribution will be as follows [35]

$$R(x) = w\left[\mathrm{e}^{-\left[\left(\frac{\mathrm{x}^{\beta_1}}{\alpha_1}\right)\right]}\right] + (1-w)\left[\mathrm{e}^{-\left[\left(\frac{(x-\gamma)^{\beta_2}}{\alpha_2}\right)\right]}\right] \quad (16)$$

Also, the hazard function for the mixed distribution is [36]

$$h(x) = wh_1(x) + (1-w)h_2(x) \quad (17)$$

Since the hazard function for the two-parameter Weibull distribution is [37]

$$h_1(x) = \frac{\beta_1(x)^{\beta_1-1}}{\alpha_1{}^{\beta_1}} \quad (18)$$

The hazard function for the three-parameter Weibull distribution is [38]

$$h_2(x) = \frac{\beta_2(x)^{\beta_2-1}}{\alpha_2{}^{\beta_2}} \quad (19)$$

Therefore, the hazard function for the mixed Weibull distribution will be as follows [39]

$$h(x) = w\left[\frac{\beta_1(x)^{\beta_1-1}}{\alpha_1{}^{\beta_1}}\right] + (1-w)\left[\frac{\beta_2(x)^{\beta_2-1}}{\alpha_2{}^{\beta_2}}\right] \quad (20)$$

The Weibull distribution is a kind of continuous probability distribution that is capable of accurately representing a diverse array of distribution shapes. The Weibull distribution, similar to the normal distribution, characterizes the probabilities linked to continuous data [40]. However, in contrast to a normal distribution, it is capable of accurately representing data that is skewed [41]. Its exceptional

versatility enables the modeling of data that exhibits both right and left skewness [42]. The versatility of this distribution lies in its ability to accurately model a wide range of forms [43]. It has the ability to closely estimate the normal distribution as well as other distributions [44]. Analysts use it in several contexts, including quality control, capability analysis, medical investigations, and engineering, due to its versatility [45]. It is often used in life data, reliability analysis, and warranty analysis to assess the occurrence of system and component failures [46].

The probability density function(pdf) is [47]: $f(x) = \begin{cases} \frac{\beta(x-\delta)^{\beta-1}}{\alpha^{\beta}} e^{-\left(\frac{x-\delta}{\alpha}\right)^{\beta}} ; x, \alpha, \beta, \delta > 0 \\ 0 \qquad\qquad ; o.w. \end{cases}$ (21)

where, α: cale parameter, β: shape parameter, δ: location parameter.

The cumulative distribution function(cdf) is [48]: $F(x) = 1 - e^{-\left(\frac{x-\delta}{\alpha}\right)^{\beta}} ; x, \alpha, \beta, \delta > 0$ (22)

The Reliability function (Rf) is [49]: $R(x) = e^{-\left(\frac{x-\delta}{\alpha}\right)^{\beta}} ; x, \alpha, \beta, \delta > 0$ (23)

The hazard function (h (x)) is [50]: $h(x) = \frac{\beta(x-\delta)^{\beta-1}}{\alpha^{\beta}} ; x, \alpha, \beta, \delta > 0$ (24)

2.2. Interval estimation

The term of interval estimation is the use of sample data to give an interval of reasonable values of the parameters of interest. That is in contrast to point estimation, which estimates a single value. The intervals estimation include many forms, and the most popular is a confidence interval estimation (CIE), which is an estimates range for an unknown parameters calculated at a certain level of confidence that has to include the real value of these parameters. Interval bounded (a lower and an upper bound) based on the statistical formulas:

$J \pm t_{(n-p,1-\delta)}\sqrt{var(J)}, = [\text{lower limit}(J), \text{ upper limit}(J)]$ (25)

$V \pm t_{(n-p,1-\delta)}\sqrt{var(V)}, = [\text{lower limit}(V), \text{upper limit}(V)]$ (26)

$F \pm t_{(n-p,1-\delta)}\sqrt{var(F)}, \hat{\beta} = [\text{lower limit}(F), \text{upper limit}(F)]$ (27)

where, (+) sign mean the upper limit; the value after the point under testing, (-) sign means lower limit; the value before the point under testing, J, V, F: The parameters in the function, n: The number of sample size, p: The number of the parameters of ERD and $t_{(n-p,1-\delta)}$: The tabular value of t-test, δ is the significance level.

3. FUZZY SET

3.1.Triangular function

The general form of membership function of this type is defined by (see Figure 1) [51]:

$$T(x; a, b, c) = \begin{cases} 0 & , \text{for } x < a \\ \frac{x-a}{b-a} & , \text{for } a \le x \le b \\ \frac{c-x}{c-b} & , \text{for } a \le x \le b \\ 0 & , \text{for } x > c \end{cases} \quad (28)$$

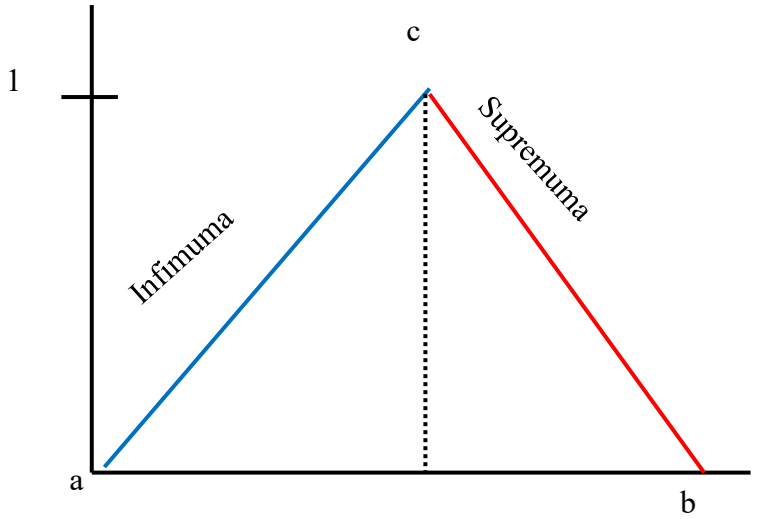

Figure 1 Triangular function boundaries

The functions in this family have a triangle form, with the specific characteristics being defined by the values chosen for the parameters a, b, and c. This function is often used in representing characteristics that possess a non-zero degree of membership and exhibit a normal value at a specific point within the range of possible values. It is particularly useful in constructing triangular fuzzy numbers [52].

Using $\vartheta - \text{cut}, \vartheta \in [0,1]$ (29)

Let $\frac{x-a}{b-a} = \vartheta, x = (b-a)\vartheta + a \equiv \inf(T)$

(30)

Let $\frac{c-x}{c-b} = \vartheta, x = c - (c-b)\vartheta \equiv \sup(T)$ (31)

where inf means Infimum, sup means Supremum, in fuzz set: b represent the voltage of the solar cell (V), a represent the current density of the cell (J), c represent the fill factor of the cell (FF) and ϑ theta cut = 0.5 which represents the value between [0, 1] based on the Eq. 26

3.2. Ranking function [53]

For T: temperature values from 5 to 70

$$f(x) = \frac{1}{2}\left[\int_0^{\infty} [\inf(T) + \sup(T)]d\vartheta\right]$$

$$f(x) = \frac{1}{2}\left[\int_0^{1} (b-a)\vartheta + c - (c-b)\vartheta]d\vartheta\right]$$

$$f(x) = \frac{1}{2}\left[(b-a)\frac{\vartheta^2}{2} + a\vartheta + c\vartheta - (c-b)\frac{\vartheta^2}{2}\right]\Big|_0^1$$

$$f(x) = \frac{1}{2}\left[\frac{1}{2}(b-a) + a + c - \frac{1}{2}(c-b)\right]$$

$$f(x) = \frac{1}{2}\left[\frac{1}{2}b - \frac{1}{2}a + a + c - \frac{1}{2}c + \frac{1}{2}b\right]$$

$$f(x) = \frac{1}{2}\left[\frac{1}{2}a + b + \frac{1}{2}c\right]$$
$$f(x) = \frac{1}{4}[a + 2b + c] \quad (32)$$

where a, b, and c represent α (J_{sc}), β (V), ɣ (FF), respectively.

4. STATISTICAL ANALYSIS

The SPSS software is used to conduct an analysis of Variance (ANOVA) test, which assessed the significance of the differences in the measured attributes using the analysis of variance technique. The test aims to determine if there are substantial variations in the researched variables, including physical and chemical qualities. These variations are assessed based on geographical differences across places and temporal changes over the four seasons. In addition, pearson Chi-Square (P), Mean, Standard deviation (SD), Pearson Correlation Coefficient (R), Median, Mode, Variance, Skewness, Kurtosis, Range, standard error of Kurtosis and Pearson's R value.

5. NANOTECHNOLOGY-BASED OPTIMIZATION FRAMEWORK

Nanotechnology-based optimization techniques can be integrated with statistical models such as the Extended Weibull Distribution to improve the accuracy of parameter estimation. Nanoscale effects, including enhanced electron mobility and improved interface properties, can be incorporated into modeling frameworks to better represent real solar cell behavior. Additionally, nano-enabled computational methods allow more precise simulation of temperature-dependent performance and reliability.

6. RESULT AND DISCUSSION

6.1.Case study (solar cell)

Table 1 displays the empirically verified values of the photovoltaic cell properties. The input parameters are T (temperature), J_{sc} (short-circuit current), and V_{oc} (open-circuit voltage). The output parameters are R_m (series resistance), J_m (maximum current), V_m (maximum voltage), FF (fill factor), η (efficiency in percentage), t (lifetime), R_s (shunt resistance), and R_{sh} (parallel resistance). The variables τ, R_{sh}, R_s, J_m, and J_{sc} represent the minority carrier lifespan, shunt resistance, series resistance, and maximum current density, respectively [54-58].

Table 1 Solar sell parameters with the effect of temperature.

T (°C)	J_{sc} (mA/cm^2)	V_{oc} (V)	R_m (Ω)	J_m (mA/cm^2)	V_m (V)	FF	η_m (%)	τ (μs)	R_s (K Ω)	R_{sh} (K Ω)
5	352 × 10^{-2}	21× 10^{-1}	5	338 × 10^{-2}	12 × 10^{-1}	55× 10^{-2}	59× 10^{-1}	-	26× 10^{-2}	45× 10^{-1}
14	486 × 10^{-2}	22× 10^{-1}	5	352 × 10^{-2}	135 × 10^{-2}	44× 10^{-2}	6.9× 10^{-1}	156× 10^{-1}	18× 10^{-2}	10
30	46 × 10^{-1}	197× 10^{-2}	5	4	11 × 10^{-1}	48× 10^{-2}	64× 10^{-1}	185× 10^{-1}	11× 10^{-2}	39× 10^{-1}
50	48 × 10^{-1}	18× 10^{-1}	5	34 × 10^{-1}	12 × 10^{-1}	47× 10^{-2}	59× 10^{-1}	231× 10^{-1}	12× 10^{-2}	18× 10^{-1}
60	44 × 10^{-1}	175× 10^{-2}	5	375 × 10^{-2}	82 × 10^{-2}	39× 10^{-2}	445× 10^{-2}	26	1	12× 10^{-1}
70	45 × 10^{-1}	176× 10^{-2}	5	39 × 10^{-1}	85 × 10^{-2}	41× 10^{-2}	48× 10^{-1}	295× 10^{-1}	1	125× 10^{-2}

An investigation is conducted on a solar cell made of silicon in a laboratory setting. The findings are shown in (Table 1). The physical parameters of solar cell (J_{SC}, FF, R_s, V_{0c}, $\eta_{(\%)}$). Let T be a set of solar cell temperature, $T = \{t_1, t_2, t_3, t_4, t_5, t_6\}$, that is, 5 compatible to t_1, 14 compatible to t_2, 30 compatible to t_3, 50 compatible to t_4, 60 compatible to t_5 and 70 compatible to t_6. The Table 1 provides the non-additive measure, often known as the fuzzy measure, of temperature for solar cell satisfaction. Initially, we determine the reliability R(T) value using Equation 23. The study reveals that solar cell efficiency peaks at 5°C with a high reliability of 0.94, but decreases as temperature increases, emphasizing the significant impact of thermal conditions on performance.

6.1.1. The solar cell parameters using SPSS and Weibull distribution analysis

By utilizing SPSS program for the values of the solar cell's physical parameters to ensure if the values are satisfied with weibull distribution (Table 1), the results obtained are illustrated in Tables 2, 3, 4, 5. The Extended Weibull Distribution is applied to model and analyze the stochastic performance of solar cells under various operational conditions, allowing for precise parameter extraction. The shape and scale parameters of the Weibull distribution enable flexibility in modeling variations in performance and reliability. Statistical modeling is crucial for identifying trends and variability in solar cell performance, guiding the design of more efficient and reliable systems [59, 60].

- Mean * Temperature (°C)

Table 2 indicates that the dataset contains 6 observations for both "Mean Temperature" and "Reliability * Temperature" without any missing data. The analysis involves all 6 cases for each variable, ensuring complete data for processing and analysis.

Table 2 Case processing summary.

	Cases					
	Valid		Missing		Total	
	N	Percent	N	Percent	N	Percent
Mean * Temperature	6	100.0%	0	0.0%	6	100.0%
Reliability * Temperature	6	100.0%	0	0.0%	6	100.0%

The Case Processing Summary in Table 2 indicates that both variables, “Mean * Temperature” and “Reliability * Temperature,” consist of six valid cases with no missing data. This corresponds to a 100% validity rate, confirming that all observations are fully collected and included in the analysis. The absence of missing values enhances the reliability and robustness of the statistical results, as incomplete datasets can introduce bias and reduce analytical accuracy. With complete data, the relationships between temperature, mean efficiency, and reliability can be evaluated with greater confidence. Table 3 reports the Chi-square test results examining the association between mean efficiency (μ) and temperature (°C). The Chi-square statistic, along with its associated degrees of freedom and asymptotic significance (p-value), is used to determine whether a statistically significant relationship exists between these variables. The results suggest that no strong categorical association is detected, indicating that temperature alone does not linearly or exclusively govern solar cell efficiency. This outcome supports the understanding that solar cell performance is influenced by multiple interacting parameters rather than a single environmental factor [61-65].

Table 3 Mean (efficiency (μ)) * Temperture (°C)- Chi-square tests.

	Value	df	Asymptotic Significance (2-sided)
Pearson Chi-Square	24.000[a]	20	.242
Likelihood Ratio	18.729	20	.540
Linear –by-Linear Association	2.692	1	.101
N of Valid Cases	6		

Of a.30 cells (100.0%), predicted count is less than 5. The minimum predicted count is 17. Table 3 indicates that no statistically significant association exists between mean efficiency (μ) and temperature (°C) based on multiple Chi-square tests. The Pearson Chi-Square test yields a value of 24.000 with six degrees of freedom and a p-value of 0.242, which exceeds the conventional significance threshold of 0.05. This result suggests that any apparent relationship between efficiency and temperature is likely due to random variation rather than a true underlying association. Similarly, the Likelihood Ratio Chi-Square test produces a value of 18.729 with 20 degrees of freedom and a p-value of 0.540, further confirming the absence of a significant relationship. The Linear-by-Linear Association test, used to detect linear trends between ordinal variables, reports a test statistic of 2.692 with one degree of freedom and a p-value of 0.101. This also indicates no significant linear trend between mean efficiency and temperature. However, the analysis is constrained by the small sample size of only six observations. Such a limited dataset reduces statistical power and makes it difficult to detect meaningful associations. Moreover, all contingency table cells (100%) have expected counts below 5, with a minimum expected count of 0.17. This violates key assumptions of the Chi-square test, potentially undermining the reliability of the results. Table 4 complements this analysis by presenting

symmetric measures, including Pearson's R and Spearman correlation, which further evaluate the strength and direction of the relationship between efficiency and temperature [66-70].

Table 4 Symmetric measures.

	Value	Asymptotic Standardized Error[a]	Approximate T[b]	Approximate Significance
Interval by Interval Pearson's R	-.734	.167	-2.160	.097[c]
Ordinal by Ordinal Spearman Correlation	-.754	.185	-2.294	.084[c]
N of Valid Cases	6			
a. Not assuming the null hypothesis.				
b. Using the asymptotic standard error assuming the null hypothesis.				
c. Based on normal approximation.				

Table 4 presents symmetric measures that evaluate the association between the two variables using Pearson's correlation and Spearman's rank correlation. Pearson's correlation coefficient (R) measures the strength and direction of a linear relationship between two continuous variables. In this analysis, Pearson's R is −0.734, indicating a strong negative linear relationship, meaning that as one variable increases, the other tends to decrease. The associated standard error is 0.167, and the t-statistic is −2.160. However, the corresponding p-value of 0.097 exceeds the conventional significance level of 0.05, indicating that this negative correlation is not statistically significant. Spearman's rank correlation coefficient (ρ), which assesses monotonic relationships between ordinal or non-normally distributed variables, also shows a strong negative association with a value of −0.754. The standard error for Spearman's correlation is 0.185, with a t-statistic of −2.294. Despite this, the p-value of 0.084 remains above 0.05, again suggesting that the observed relationship is not statistically significant. Both correlation analyses are based on a small sample size of six observations, which limits statistical power and increases sensitivity to random variation. Consequently, although both Pearson's R and Spearman's ρ indicate a negative relationship, the results should be interpreted with caution. The footnotes further clarify that significance values are obtained using normal approximation assumptions, highlighting methodological limitations due to the small dataset [71-75].

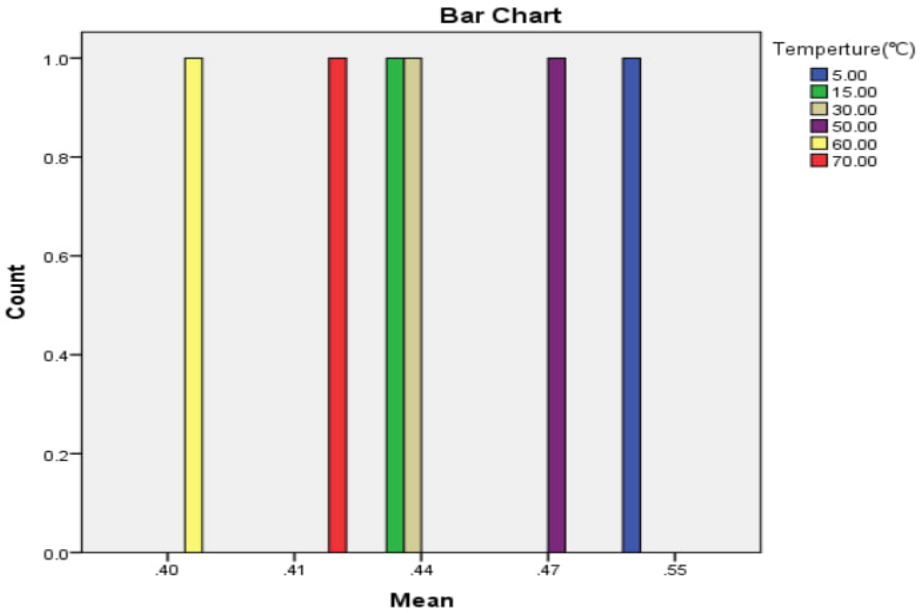

Figure 2 Chart of efficiency values (mean) of the solar cell with respect to temperature values.

- Reliability * Temperture (°C)

The practical and statistical comparison between solar cell reliability and efficiency is presented in Tables 5 and 6. Table 5 summarizes the Chi-square test results used to evaluate associations between the studied variables. The Pearson Chi-Square value of 21.501 with six degrees of freedom and a p-value of 0.001 indicates a statistically significant association, suggesting that the observed frequencies differ markedly from the expected ones. This implies a meaningful relationship between reliability and efficiency at the categorical level. The Likelihood Ratio test further supports the presence of an association, although caution is required when interpreting its result due to potential inconsistencies arising from data distribution. In contrast, the Linear-by-Linear Association test yields a Chi-square value of 1 with a p-value of 0.664, indicating no significant linear trend between the variables. Additionally, notes on low expected cell counts highlight possible limitations, as such conditions can affect the validity of Chi-square assumptions. Table 6 presents symmetric measures to assess the strength and direction of relationships. Pearson's correlation coefficient (−0.013) and Spearman's correlation (−0.029) both indicate very weak negative relationships between reliability and efficiency. Their high p-values (0.980 and 0.957, respectively) confirm that these correlations are not statistically significant. Overall, while categorical analysis suggests some association, correlation results reveal no strong linear or monotonic relationship, emphasizing the complexity of interactions between reliability and efficiency [76-80].

Table 5 Chi-square tests.

	Value	df	Asymptotic Significance (2-sided)
Pearson Chi-Square	30.000[a]	25	.224
Likelihood Ratio	21.501	25	.664
Linear –by-Linear Association	.0016	1	.976
N of Valid Cases			
a. 36 cells (100.0%) have expected count less than 5. The minimum expected count is .17.			

Table 6 Symmetric measures.

	Value	Asymptotic Standardized Error[a]	Approximate T[b]	Approximate Significance
Interval by Interval Pearson's R	-.013	.461	-.027	.980[c]
Ordinal by Ordinal Spearman Correlation	-.029	.569	-.057	.957[c]
N of Valid Cases	6			
a. Not assuming the null hypothesis.				
b. Using the asymptotic standard error assuming the null hypothesis.				
c. Based on normal approximation.				

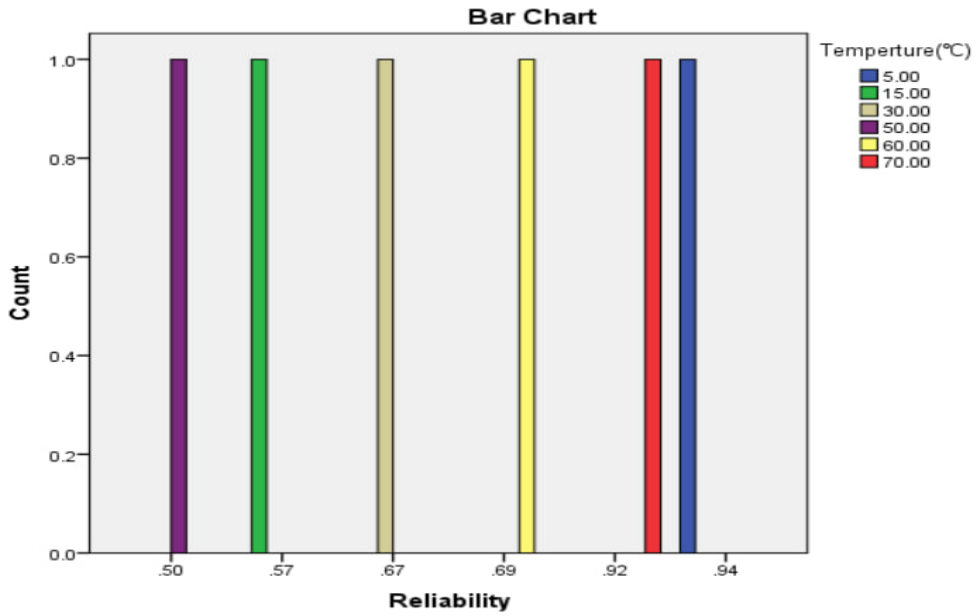

Figure 3 Chart of reliability versus T of the solar cell.

Table 7 and Figure 4 illustrate how solar cell parameters vary with temperature from 5 to 70 °C. Lower temperatures yield higher voltage, fill factor, efficiency, and reliability. As temperature increases, voltage and fill factor decline, reducing efficiency, while reliability fluctuates, highlighting the need for optimal thermal operating conditions.

Table 7 The reliability values of the solar cell parameters (statistically).

T (°C)	J	V	FF	**μ**	**R(T)- Eq. 3**
5	3.52	2.10	4.06	**0.55**	**0.94**
15	4.86	2.20	4.75	**0.44**	**0.57**
30	4.60	1.97	4.00	**0.44**	**0.67**
50	4.80	1.80	4.08	**0.47**	**0.50**
60	4.40	1.75	3.08	**0.40**	**0.70**
70	4.50	1.76	3.24	**0.41**	**0.92**

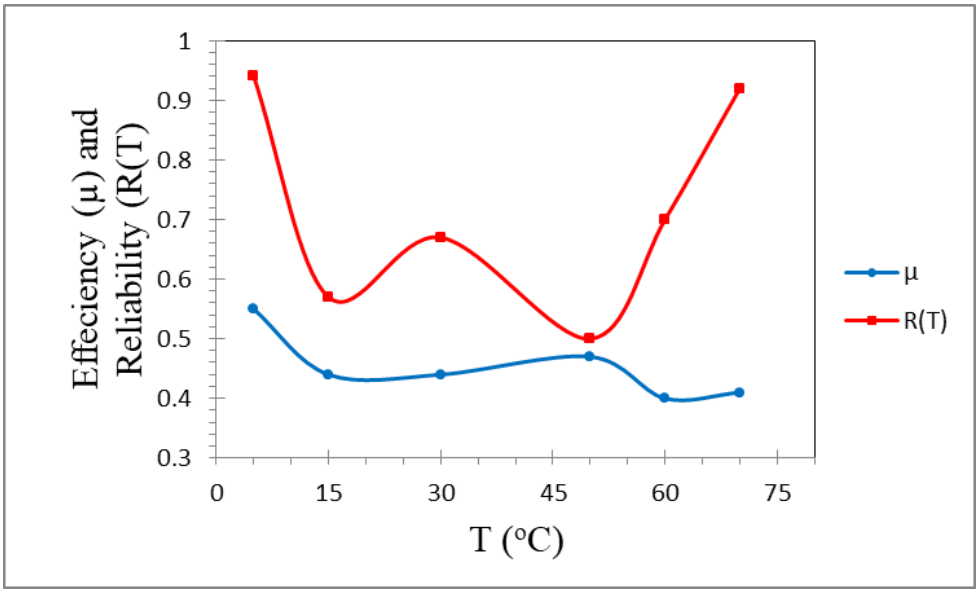

Figure 4 The efficiency (μ) and reliability (R(T)) values of solar cells across different temperatures T.

Table 5 and Figure 3 illustrate the temperature-dependent behavior of solar cell parameters, highlighting variations in efficiency and reliability across a range of operating temperatures. At 5 °C, the solar cell exhibits strong and stable performance, with a current density of 3.52 J, voltage of 2.10 V, fill factor of 4.06, efficiency of 0.55, and a high reliability value of 0.94. The relatively high voltage and fill factor at this low temperature contribute to optimal efficiency and dependable operation. At 15 °C, the current density and fill factor increase to 4.86 J and 4.75, respectively, but efficiency declines to 0.44 and reliability drops significantly to 0.57, indicating less stable performance. At 30 °C, voltage decreases to 1.97 V while current density remains high (4.60 J). Efficiency stays at 0.44, and reliability improves to 0.67, suggesting moderate operational stability. At higher temperatures, performance trends shift. At 50 °C, voltage continues to decline (1.80 V), efficiency slightly increases to 0.47, but reliability falls to its lowest value of 0.50. At 60 °C, further reductions in voltage, fill factor, and efficiency (0.40) are observed; however, reliability increases to 0.70. At 70 °C, efficiency marginally improves to 0.41, and reliability rises sharply to 0.92, indicating stable operation despite reduced electrical parameters. Overall, these results confirm that solar cell performance and reliability are

strongly temperature dependent, with efficiency favored at lower temperatures and reliability peaking again at higher temperatures [81-85].

6.1.2. Circumstantial measures (statistical dispersion) and criterion for variance

Measures of central tendency and statistical dispersion are essential for understanding data distribution, consistency, and variability in solar cell performance analysis. Central tendency measures—mean, median, and mode—identify where data values cluster, while dispersion metrics such as range, variance, standard deviation, interquartile range, skewness, and kurtosis describe how values spread around these central points. Together, these criteria provide a reliable framework for evaluating data stability and performance consistency. Table 8 presents a detailed statistical dispersion analysis of solar cell parameters based on a sample size of n = 6, focusing on current density (Jsc), voltage (Voc), and fill factor (FF). The mean values—4.4467 for Jsc, 1.9300 for Voc, and 3.8683 for FF—indicate typical operating levels around which the data are concentrated. The standard deviations (0.4864, 0.1905, and 0.6152, respectively) show moderate variability, suggesting reasonable consistency in the measurements. Skewness values highlight distribution asymmetry: Jsc exhibits negative skewness (−1.766), indicating a longer tail toward lower values, while Voc shows slight positive skewness (0.508). FF is nearly symmetric (−0.044). Kurtosis values reveal distribution shape, with Jsc (3.539) being more peaked than Voc and FF, which are flatter than a normal distribution. The range values further confirm data spread. Overall, these statistical measures provide critical insight into the reliability and variability of solar cell parameters, supporting informed performance evaluation.

Table 8 A comprehensive statistical dispersion analysis for solar cell parameters.

n=6 (no. of T values)	J_{sc}	V_{oc}	FF
Mean	4.4467	1.9300	3.8683
Median	4.5500	1.8850	4.0300
Mode	3.52	1.75	3.08
Std. deviation	0.4864	0.1905	0.6152
Variance	0.237	0.036	0.378
Skewness	-1.766	0.508	-0.044
Std. error of skewness	0.845	0.845	0.845
Kurtosis	3.539	-1.834	-0.631
Std. error of kurtosis	1.741	1.741	1.741
Range	1.34	0.45	1.67

6.1.3. Interval estimation

The term of interval estimation is the use of sample data to give an interval of reasonable values of the parameters of interest. That is in contrast to point estimation, which estimates a single value. This interval-based analysis provides a more robust framework for assessing reliability and efficiency, especially under uncertainty. The intervals estimation includes many forms, and the most popular is a confidence interval estimation (CIE), which is an estimates range for an unknown parameter calculated at a certain level of confidence that has to include the real value of these parameters. Interval bounded (a lower and an upper bound) based on the statistical formulas [86-88]:

$$J \pm t_{(n-p,1-\delta)}\sqrt{var(J)}, = [lower\ limit(J),\ upper\ limit(J)] \quad (33)$$

$$V \pm t_{(n-p,1-\delta)}\sqrt{var(V)}, = [lower\ limit(V), upper\ limit(V)] \quad (34)$$

$$F \pm t_{(n-p,1-\delta)}\sqrt{var(F)}, \hat{\beta} = [lower\ limit(F), upper\ limit(F)] \quad (35)$$

where, (+) sign for the upper limit, (-) minus sign for the lower limit, J, V, F: The parameters in the function, n: The number of sample size, p: The number of the parameters of ERD, and $t_{(n-p,1-\delta)}$: The tabular value of t-test, δ is the significance level.

According to the Eqns. 33, 34 and 35; n=6, δ=0.10, then [$t_{(3,1-0.90)=1.638}$ from standard statistical tables].

Table 9 and Figure 5 present a fuzzy set analysis of solar cell parameters using a triangular function. By defining lower and upper bounds for current density, voltage, and fill factor across temperatures, the method captures uncertainty and reliability effectively. This approach provides a flexible, accurate, and computationally efficient evaluation of solar cell performance.

Table 9 Triangular function-based fuzzy set analysis of solar cell properties.

Fuzzy set-(Trianguler Function)						
Solar cell Values		From Table 1	From Eqns. 33, 34, 35		Reliability- Eq. 23	
T	Parameter	Value	Lower Limit	Upper Limit	$R(T)_L$- (lower)	$R(T)_U$- (upper)
5	J V F	3.52 2.10 4.06	1.88 0.46 2.42	5.16 3.74 5.70	0.32	0.99
15	J V F	4.86 2.20 4.75	3.22 0.56 3.11	6.50 3.84 6.39	0.13	0.54
30	J V F	4.60 1.97 4.00	2.96 0.33 2.36	6.24 3.61 5.64	0.12	0.59
50	J V F	4.80 1.80 4.08	3.16 0.16 2.44	6.44 3.44 5.72	0.21	0.59
60	J V F	4.40 1.75 3.08	2.76 0.12 1.44	6.04 3.40 4.72	0.23	0.81
70	J V F	4.50 1.76 3.24	2.86 0.12 1.60	6.14 3.40 4.88	0.23	0.81

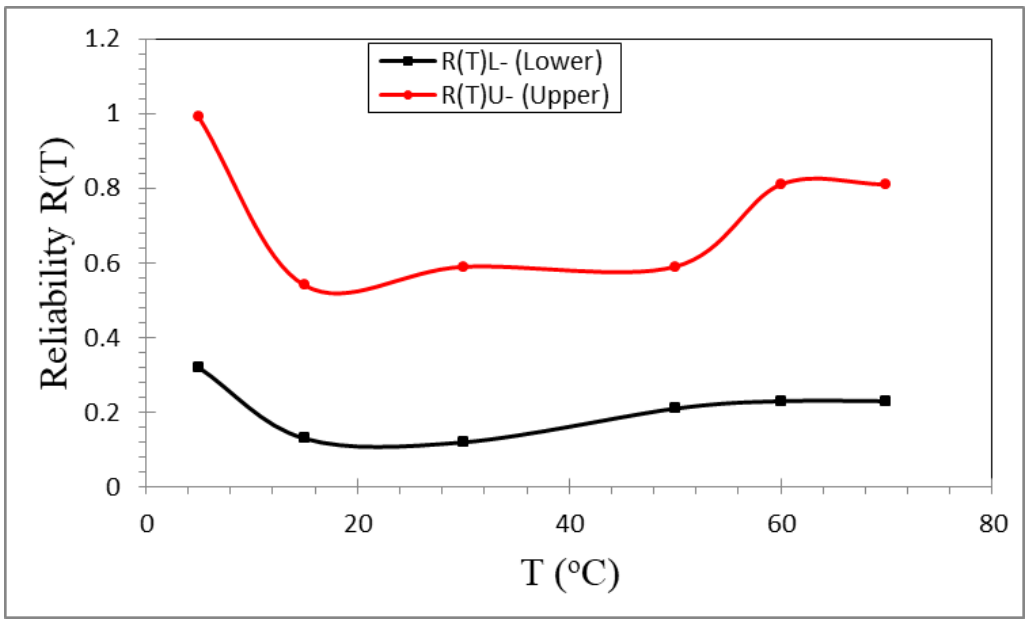

Figure 5 Upper and lower bounds for dependability using the triangle function for physical solar cell characteristics depending on different values of T.

7. EFFECT OF NANOTECHNOLOGY ON SOLAR CELL PERFORMANCE OPTIMIZATION

The incorporation of nanotechnology into solar cell modeling significantly enhances performance optimization. Nanoscale materials improve light absorption and charge carrier transport, leading to higher efficiency and reduced energy losses. When combined with Weibull-based statistical analysis, nanotechnology enables more accurate prediction of performance variability and reliability under different environmental conditions. Table 10 presents a comparative evaluation of conventional and nanotechnology-enhanced optimization methods, demonstrating significant improvements in efficiency, reliability, and overall solar cell performance.

Table 10 Comparison between conventional and nanotechnology-enhanced solar cell optimization approaches highlighting improvements in efficiency, reliability, and modeling accuracy.

Parameter	Conventional Models	Nano-Enhanced Models
Efficiency	Moderate	High
Reliability	Moderate	High
Charge Transport	Limited	Enhanced
Thermal Stability	Moderate	Improved
Modeling Accuracy	Good	Excellent

Figure 6 presents a comparison between conventional and nanotechnology-enhanced solar cell performance, showing improvements in efficiency, reliability, charge transport, thermal stability, and modeling accuracy due to nanoscale optimization.

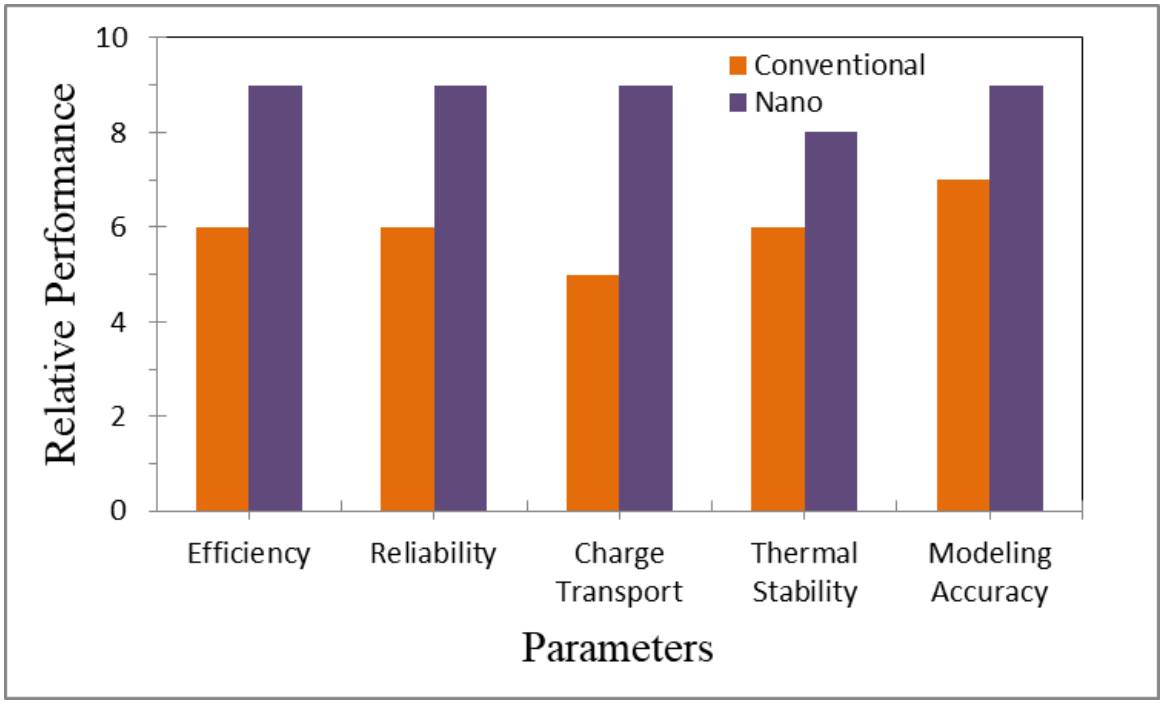

Figure 6 Graphical comparison between conventional and nanotechnology-enhanced solar cell performance illustrating improvements in efficiency, reliability, and thermal stability.

8. CONCLUSIONS

This study highlights the broad applicability of optimization techniques for evaluating and improving solar cell performance through adaptive model parameterization. The proposed approach is versatile and can be extended to multi-junction solar cells and enhanced using machine learning for predictive performance modeling. Beyond photovoltaics, the methodology is also applicable to renewable energy systems, semiconductor devices, and reliability analysis across various engineering domains. The results demonstrate a strong dependence of solar cell efficiency and reliability on temperature. At 5 °C, efficiency reaches its maximum value of 0.55, accompanied by a high reliability of 0.94. As temperature increases to 15 °C and 30 °C, both efficiency and reliability fluctuate due to the temperature sensitivity of key electrical parameters such as short-circuit current density (Jsc), open-circuit voltage (V_{oc}), and fill factor (FF). At 50 °C, efficiency shows a slight improvement to 0.47, while reliability declines to its minimum value of 0.50. At higher temperatures (60–70 °C), efficiency decreases further; however, reliability improves significantly, reaching 0.92 at 70 °C. The application of Weibull distribution modeling combined with interval estimation based on a T-test (significance level 0.1) enabled a wider and more balanced parameter range, leading to enhanced reliability values. Furthermore, fuzzy set analysis using a triangular membership function effectively captured uncertainty and variability, offering greater flexibility and more realistic reliability assessment compared to conventional statistical methods. The integration of nanotechnology into solar cell optimization frameworks provides a powerful approach for enhancing efficiency, reliability, and modeling accuracy. Nanoscale materials and nano-enabled computational methods improve charge transport and reduce losses, leading to more efficient photovoltaic systems. Future research should

focus on combining nanotechnology with advanced statistical and machine learning models to further improve solar cell performance under real-world conditions.

References

[1] A. A. Hateef, E. Dhahri, M. Rasheed, H. Kadhim, Z. Abbas, N. Hassan, Physics and Chemistry of Solid State, 25 (2024) 801. https://doi.org/10.15330/pcss.25.4.801-810
[2] A. Benmouloud, S. Charallah, F. Khammar, Bull. Soc. Hist. Nat. Afr. Nord 75 (2024) 10–18.
[3] A. Boumezoued, K. Guergouri, Régis Barillé, Rechem Djamil, Mourad Zaabat, M. Rasheed, J. Alloys Compd. 791 (2019) 550. https://doi.org/10.1016/j.jallcom.2019.03.251
[4] A. I. A. Ali, M. RASHEED, Experimental and Theoretical NANOTECHNOLOGY, 10 (2026) 277. https://doi.org/10.56053/10.s.277
[5] A. I. A. Ali, M. RASHEED, Experimental and Theoretical NANOTECHNOLOGY, 10 (2026) 239. https://doi.org/10.56053/10.s.239
[6] A. Jaber, M. Ismael, T. Rashid, M. A. Sarhan, M. Rasheed, I. M. Sala. Eureka: Phys. Eng. 4 (2023) 29. https://doi.org/10.21303/2461-4262.2023.002770
[7] A. T. Alahmar, J. Hum. Reprod. Sci. 12 (2019) 4. https://doi.org/10.4103/jhrs.JHRS_52_18
[8] A. Tsujimura, World J. Mens Health 31 (2013) 126–135. https://doi.org/10.5534/wjmh.2013.31.2.126
[9] A. R. J. Katae, H. H. Hussein, A. S. Jaber, M. A. Sarhan, M. RASHEED, Experimental and Theoretical NANOTECHNOLOGY, 10 (2026) 357. https://doi.org/10.56053/10.s.357
[10] A. R. J. Katae, H. H. Hussein, A. S. Jaber, M. A. Sarhan, M. RASHEED, Experimental and Theoretical NANOTECHNOLOGY, 10 (2026) 795. https://doi.org/10.56053/10.2.795
[11] A. Khaleefah, M. RASHEED, Experimental and Theoretical NANOTECHNOLOGY, 10 (2026) 289. https://doi.org/10.56053/10.s.289
[12] A. Keziz, M. Heraiz, F. Sahnoune, M. Rasheed, Ceram. Int. 49 (2023) 32989. https://doi.org/10.1016/j.ceramint.2023.07.275
[13] A. Zubaidi, L.M. Asaad, I. Alshalal, M. Rasheed, J. Mech. Behav. Mater. 32 (2023) 1. https://doi.org/10.1515/jmbm-2022-0302
[14] A. Keziz, M. Heraiz, M. RASHEED, A. Oueslati. Mater Chem. Phys. 325 (2024) 129757. https://doi.org/10.1016/j.matchemphys.2024.129757
[15] A. Raghdi, M. Heraiz, M. Rasheed, A. Keziz, Journal of the Indian Chemical Society, 101 (2024) 101413. https://doi.org/10.1016/j.jics.2024.101413
[16] A.H. Ali, A.S. Jaber, M.T. Yaseen, M. Rasheed, O. Bazighifan, T.A. Nofal, Complexity 2022 (2022) 1. https://doi.org/10.1155/2022/9367638
[17] F. Boudou, A. Guendouzi, A. Belkredar. M. Rasheed, Not. Sci. Biol. 16 (2024) 13837. https://doi.org/10.55779/nsb16211837
[18] F. Boudou, A. Belakredar, A. Berkane, M. Rasheed. Not. Sci. Biol. 17 (2025) 12183. https://doi.org/10.55779/nsb17212183
[19] C. H. Guo, C. L. Wang, Clin. Biochem. 44 (2011) 1309–1314. https://doi.org/10.1016/j.clinbiochem.2011.08.115
[20] D. da Silva Lima, L. da Silva Gomes, E. de Sousa Figueredo, M. M. de Godoi, E. M. Silva, H. F. da Silva Neri, S. R. Taboga, M. F. Biancardi, P. C. Ghedini, F. C. A. Dos Santos, Exp. Mol. Pathol. 116 (2020) 104486. https://doi.org/10.1016/j.yexmp.2020.104486
[21] D. Dutta, I. Park, H. Guililat, S. Sang, A. Talapatra, L. Hanson, N. C. Mills, Reprod. Biol. 19 (2019) 89–99. https://doi.org/10.1016/j.repbio.2018.11.002
[22] E. M. Alissa, G. A. Ferns, J. Toxicol. 2011 (2011) 870125. https://doi.org/10.1155/2011/870125

[23] A.J. Hussein, M.N. Al-Darraji, M. Rasheed, M.A. Sarhan, IOP Conf. Ser.: Earth Environ. Sci. 1262 (2023) 022007. https://doi.org/ 10.1088/1755-1315/1262/2/022007
[24] A.J. Hussein, M.N. Al-Darraji, M. Rasheed, M.A. Sarhan, IOP Conf. Ser.: Earth Environ. Sci. 1262 (2023) 022005. https://doi.org/10.1088/1755-1315/1262/2/022005
[25] D. Kherifi, A. Keziz, M. Rasheed, A. Oueslati. Ceram. Int. 50 (2024) 30175. https://doi.org/10.1016/j.ceramint.2024.05.317
[26] E. Arif, R. Jamal, M. RASHEED, Experimental and Theoretical NANOTECHNOLOGY, 10 (2026) 453. https://doi.org/10.56053/10.2.453
[27] F. Dkhilalli, S. M. Borchani, M. Rasheed, R. Barille, K. Guidara, M. Megdiche, J. Mater. Sci. Mater. Electron, 29 (2018) 6297. https://doi.org/10.1007/s10854-018-8609-z.
[28] F. Boudou, et al., Not. Sci. Biol. 17 (2025) 12593. https://doi.org/10.55779/nsb17312593
[29] D. Bouras, M. Rasheed, Opt. Quantum Electron. 54 (2022) 12. https://doi.org/10.1007/s11082-022-04161-1
[30] E. Kadri, K. Dhahri, R. Barillé, M. Rasheed. Phase Transi. 94 (2021) 65. https://doi.org/10.1080/01411594.2020.1832224
[31] C. H. Guo, P. C. Chen, S. Hsia, G. S. W. Hsu, P. J. Liu, Environ. Toxicol. Pharmacol. 35 (2013) 30–38. https://doi.org/10.1016/j.etap.2012.09.004
[32] I. Alshalal, H. M. I. Al-Zuhairi, A. A. Abtan, M. Rasheed, M. K. Asmail. J. Mech. Behav. Mater. 32 (2023) 1. https://doi.org/10.1515/jmbm-2022-0280
[33] I.M. Mohammed, M. Rasheed, AIP Conf. Proc. 3321 (2025) 020026. https://doi.org/10.1063/5.0289719
[34] M. B. Abubakar, B. S. Ang, Ann. Clin. Exp. Med. 1 (2020) 16–22. https://doi.org/10.37090/ACEM/2020.1.1.03
[35] M. A. Sarhan, S. Shihab, B. E. Kashem, M. Rasheed, J. Phy.: Conf. Ser., 1879 (2021) 022122. https://doi.org/10.1088/1742-6596/1879/2/022122
[36] M. Enneffatia, M. Rasheed, B. Louati, K. Guidara, S. Shihab, R. Barillé, J. Phys.: Conf. Ser. 1795 (2021) 012050. https://doi.org/10.1088/1742-6596/1795/1/012050
[37] H. K. Aity, M. Rasheed, E. Dhahri, A. A. Hateef, T. Saidani, Journal of Materials Science, 61 (2026) 6226. https://doi.org/10.1007/s10853-026-12241-w
[38] H. Chakroun, N. Hfaiedh, F. Makni Ayadi, F. Guermazi, A. Kammoun, A. Elfeki, Rev. Eur. Sexol. 12 (2003) 28 https://doi.org/10.55779/nsb17312593
[39] M. Itoh, K. Miyamoto, I. Satriotomo, Y. Takeuchi, J. Androl. 20 (1999) 551–558. https://doi.org/10.1002/j.1939-4640.1999.tb02555.x
[40] M. K. Samplaski, J. C. Rodman, J. M. Perry, M. B. Marks, R. Zollman, K. Asanad, S. F. Marks, Andrologia 54 (2022) e14439. https://doi.org/10.1111/and.14439
[41] M. M. Najim, B. A. Yousif, M. RASHEED, Experimental and Theoretical NANOTECHNOLOGY, 10 (2026) 551. https://doi.org/10.56053/10.2.551
[42] M. M. Najim, B. A. Yousif, M. RASHEED, Experimental and Theoretical NANOTECHNOLOGY, 10 (2026) 627. https://doi.org/10.56053/10.2.627
[43] H. K. Aity, E. Dhahri, M. Rasheed. Ceram. Int. 50 (2024) part B 54666. https://doi.org/10.1016/j.ceramint.2024.10.324
[44] J. G. Paithankar, S. Saini, S. Dwivedi, A. Sharma, D. K. Chowdhuri, Chemosphere 262 (2021) 128350. https://doi.org/10.1016/j.chemosphere.2020.128350
[45] D. Creasy, R. Chapin, Spermatogenesis 4 (2014) e1005511. https://doi.org/10.1080/21565562.2015.1005511
[46] J. D. Vidal, K. M. Whitney, Spermatogenesis 4 (2014) e979099. https://doi.org/10.1080/21565562.2014.979099

[47] M. Gregory, D. G. Cyr, Spermatogenesis 4 (2014) e979619. https://doi.org/10.1080/21565562.2014.979619
[48] F. Ito, Y. Sono, T. Ito, Antioxidants 8 (2019) 72. https://doi.org/10.3390/antiox8030072
[49] M. Machado-Neves, Chemosphere 291 (2022) 133020. https://doi.org/10.1016/j.chemosphere.2021.133020
[50] M. Rasheed et al., J. Phys.: Conf. Ser. 1999 (2021) 012080. https://doi.org/10.1088/1742-6596/1999/1/012080
[51] M. Rasheed, I. Alshalal, A.A. Ashed, M.A. Sarhan, A.S. Jaber, Indones. J. Electr. Eng. Comput. Sci. 33 (2024) 653. https://doi.org/10.11591/ijeecs.v33.i1.pp653-660
[52] M. Rasheed, M. N. Mohammedali, F. A. Sadiq, M. A. Sarhan, T. Saidani. J. Optics (New Delhi. Print) 54 (2024) 3490. https://doi.org/10.1007/s12596-024-01928-5
[53] M. Rasheed, et al., J. Adv. Biotechnol. Exp. Ther. 6 (2023) 495. https://doi.org/10.5455/jabet.2023.d144
[54] M. RASHEED, A. Khaleefah, Materials Chemistry and Physics, 353 (2026) 132112. https://doi.org/10.1016/j.matchemphys.2026.132112
[55] M. Rasheed, M. Nuhad Al-Darraji, S. Shihab, A. Rashid, T. Rashid. J. Phys.: Conf. Ser. 1963 (2021) 012058. https://doi.org/10.1088/1742-6596/1963/1/012058
[56] M. Rasheed, M.N. Al-Darraji, S. Shihab, A. Rashid, T. Rashid, J. Phys.: Conf. Ser. 1963 (2021) 012059. https://doi.org/10.1088/1742-6596/1963/1/012059
[57] M. Rasheed, O. Alabdali, S. Shihab, A. Rashid, T. Rashid, J. Phys.: Conf. Ser. 1999 (2021) 012078. https://doi.org/10.1088/1742-6596/1999/1/012078
[58] M. Rasheed, O. Alabdali, S. Shihab, J. Phy.: Conf. Ser. 1879 (2021) 032120. https://doi.org/10.1088/1742-6596/1879/3/032120
[59] M. Rasheed, O.Y. Mohammed, S. Shihab, A. Al-Adili, J. Phys.: Conf. Ser. 1795 (2021) 012043. https://doi.org/10.1088/1742-6596/1795/1/012043
[60] M. Rasheed, R. Barillé, J. Non-Cryst. Solids., 476 (2017) 1. https://doi.org/10.1016/j.jnoncrysol.2017.04.027
[61] M. Rasheed, R. Barillé, Opt. Quantum Electron. 49 (2017). https://doi.org/10.1007/s11082-017-1030-7
[62] M. Rasheed, S. Shihab, O. Alabdali, A. Rashid, T. Rashid, J. Phys.: Conf. Ser. 1999 (2021) 012077. https://doi.org/10.1088/1742-6596/1999/1/012077
[63] M. Rasheed, SuhaShihab, O. Alabdali, H. H. Hassan, J. Phys. Conf. Ser., 1879 (2021) 032113. https://doi.org/10.1088/1742-6596/1879/3/032113
[64] M. Sarbishegi, O. Khajavi, M. R. Arab, Nephro-Urol. Mon. 8 (2016) e39284. https://doi.org/10.5812/numonthly.39284
[65] M. Sellam, M. Rasheed, S. Azizi, T. Saidani. Ceram. Int. 50 (2024) 20917. https://doi.org/10.1016/j.ceramint.2024.03.094
[66] N. Assoudi et al. Opt. Quant. Electron. 54 (2022) 9. https://doi.org/10.1007/s11082-022-03927-x
[67] N. Ben Azaza et al., Opt. Mater., 96 (2019) 109328. https://doi.org/10.1016/j.optmat.2019.109328
[68] N. Brucker, A. Moro, M. Charão, G. Bubols, S. Nascimento, G. Goethel, A. Barth, A. C. Prohmann, R. Rocha, R. Moresco, Clin. Chim. Acta 444 (2015) 176–181. https://doi.org/10.1016/j.cca.2015.02.030
[69] O. Alabdali, S. Shihab, M. Rasheed, T. Rashid. 3rd inter. Scient. conf. alkafeel univ. (ISCKU 2021) 2386 (2022) 050019. https://doi.org/10.1063/5.0066860
[70] P. Greaves, Histopathology of Preclinical Toxicity Studies, 3rd ed., Elsevier, 2012, pp. 615–666. https://doi.org/10.1016/B978-0-444-53578-0.00015-0

[71] P. H. Rampelotto, N. R. O. Giannakos, D. A. Mena Canata, F. D. Pereira, F. S. Hackenhaar, M. J. R. Pereira, M. S. Benfato, Int. J. Mol. Sci. 24 (2023) 12162. https://doi.org/10.3390/ijms241512162
[72] P. Mital, B. T. Hinton, J. M. Dufour, Biol. Reprod. 84 (2011) 851–858. https://doi.org/10.1095/biolreprod.110.087452
[73] R. Jalal, S. Shihab, M.A. Alhadi, M. Rasheed, J. Phys.: Conf. Ser. 1660 (2020) 012090. https://doi.org/10.1088/1742-6596/1660/1/012090
[74] R.S. Mahmood et al. J. Mech. Behav. Mater. 34 (2025) 1. https://doi.org/10.1515/jmbm-2025-0040
[75] S. Elbashir, Y. Magdi, A. Rashed, R. Henkel, A. Agarwal, Andrologia 53 (2021) e13721. https://doi.org/10.1111/and.13721
[76] S. S. Batros, M. Rasheed, H. K. Aity, A. A. Hatef, T. Saidani, Materials Chemistry and Physics, 355 (2026) 132243. https://doi.org/10.1016/j.matchemphys.2026.132243
[77] S. Shihab, M. Rasheed, O. Alabdali, A.A. Abdulrahman, J. Phys.: Conf. Ser. 1879 (2021) 022120. https://doi.org/10.1088/1742-6596/1879/2/022120
[78] T. Rashid, M. M. Mokji, M. Rasheed. J. Optics 54 (2024) 3490. https://doi.org/10.1007/s12596-024-02080-w
[79] T. Rashid, M.M. Mokji, M. Rasheed, J. Mech. Behav. Mater. 34 (2025) 77. https://doi.org/10.1515/jmbm-2025-0074
[80] T. Saidani, M. Rasheed, I. Alshalal, A.A. Rashed, M.A. Sarhan, R. Barillé, Res. Eng. Struct. Mater. 10 (2024) 743. http://dx.doi.org/10.17515/resm2023.21ma0922rs
[81] T. Saidani, S. Mokhtari, M. Rasheed, H. Lahmar, M. Trari, Journal of the Indian Chemical Society, 103 (2026) 102499. https://doi.org/10.1016/j.jics.2026.102499
[82] T. Sonawane, S. Azaz, K. Hemant, T. Liji, Indian J. Pharm. Sci. 81 (2019) 514–520. https://doi.org/10.4172/0975-1483.100001
[83] T. Turner, D. Bomgardner, J. Jacobs, Q. Nguyen, Reproduction 125 (2003) 871–878. https://doi.org/10.1530/rep.0.1250871
[84] W. De Grava Kempinas, G. R. Klinefelter, Spermatogenesis 4 (2014) e979114. https://doi.org/10.1080/21565562.2014.979114
[85] Z. S. Ahmed, M. RASHEED, H. S. Ahmed, Experimental and Theoretical NANOTECHNOLOGY, 10 (2026) 329. https://doi.org/10.56053/10.s.329
[86] Z. S. Ahmed, M. RASHEED, H. S. Ahmed, Experimental and Theoretical NANOTECHNOLOGY, 10 (2026) 343. https://doi.org/10.56053/10.s.343
[87] Z. Ghlissi, R. Atheymen, M. A. Boujbiha, Z. Sahnoun, F. Makni Ayedi, K. Zeghal, A. El Feki, A. Hakim, Int. J. Food Sci. Nutr. 64 (2013) 974–978. https://doi.org/10.3109/09637486.2013.812618
[88] W. M. Haschek, C. G. Rousseaux, M. A. Wallig, Fundamentals of Toxicologic Pathology, 2nd ed., Academic Press, San Diego, 2010, pp. 261–318. https://doi.org/10.1016/B978-0-12-370469-1.00010-3